Front. Earth Sci.
https://doi.org/10.1007/s11707-025-1161-2

RESEARCH ARTICLE

Separating the decomposition rates and temperature sensitivities of soil mineral-associated and particulate organic carbon using a data-model fusion approach

Zhenghu ZHOU[1], Jingzhe ZHANG[1], Xuesen PANG[1], Lei HOU (✉)[2]

1 Key Laboratory of Sustainable Forest Ecosystem Management (Ministry of Education), School of Ecology, Northeast Forestry University, Harbin 150040, China
2 Resources and Environment College, Xizang Agricultural and Animal Husbandry University, Nyingchi 860000, China

Abstract Although soil organic carbon (SOC) is a continuum of progressively decomposed compounds with diverse molecular structures, classifying SOC into particulate organic carbon (POC) and mineral-associated organic carbon (MAOC) has been suggested to improve our understanding of SOC vulnerability to environmental changes. Incubation experiments have been extensively employed as a powerful approach to the investigation of SOC decomposition, as this method can isolate specific effects from covariations in the field. Here, we proposed a method to separate the decomposition rates and temperature sensitivities (Q_{10}) of POC and MAOC from bulk soil incubation data using the Bayesian Markov Chain Monte Carlo technique. The data used to validate our method was collected from a ~2600 m altitudinal transect in the Eastern Himalayas. We found that reactive iron plus aluminum oxides had a significant negative effect on the decomposition rate of MAOC but had no effect on the decomposition rate of POC. The negative effect of reactive iron plus aluminum oxides on Q_{10} for POC was stronger than that on Q_{10} for MAOC. In addition, the relative values of Q_{10} for POC and MAOC depended upon elevation, challenging the assumed higher Q_{10} for POC than that for MAOC from the carbon quality temperature hypothesis. Overall, the proposed approach will improve our mechanistical understanding of soil MAOC and POC dynamics in response to environmental changes.

Keywords mineral protection, mineral-associated organic carbon, particulate organic carbon, data assimilation, decomposition, temperature sensitivity

Received November 18, 2024; accepted April 1, 2025

E-mail: 465133704@qq.com

1 Introduction

Soil, a crucial component of the terrestrial ecosystem, provides multifunctionality that contributes to human welfare, such as the buildup of soil nutrients, biomass production, storage and filtration of water, carbon sequestration, habitat for soil biota, and degradation of contaminants (Schmidt et al., 2011). Carbon sequestration is a critical function of soil because it not only regulates the climate but also supports all other functions (Wiesmeier et al., 2019). Effective management of soil organic carbon (SOC) would greatly aid climate mitigation because SOC has been suggested to represent 25% of the potential of natural climate solutions (Bossio et al., 2020), requiring an ability to accurately predict SOC cycle at local to regional scales on our changing planet (Lehmann et al., 2020). Such natural climate solutions depend on a deep understanding of SOC formation, stabilization, and destabilization (Bailey et al., 2019; Wiesmeier et al., 2019; Buckeridge et al., 2020; Lavallee et al., 2020; Lehmann et al., 2020).

Although SOC is a continuum of progressively decomposed organic compounds with diverse molecular structures, the performance of a specific function of SOC is the result of the simultaneous action of SOC compounds with similar chemical, mineral, and physical properties (Lehmann and Kleber, 2015). Therefore, classification of SOC into functional groups or pools has significant implications for both experimental and modeling researches (Heckman et al., 2022; Zhou et al., 2022). For example, an acid hydrolysis approach is widely used to separate SOC into labile and recalcitrant SOC pools (Rovira and Vallejo, 2002). Soil carbon models such as Century (Parton et al., 2010) or RothC (Jenkinson and Coleman, 2008) assume that soil organic matter can be divided into pools with distinct turnover

rates. However, the advanced theory of SOC persistence highlights the critical role of physical accessibility rather than biochemical recalcitrance in dominating the decomposition of SOC. Therefore, classifying SOC into particulate organic carbon (POC) and mineral-associated organic carbon (MAOC) would improve our understanding of SOC vulnerability to environmental changes (Lavallee et al., 2020; García-Palacios et al., 2024; Zhou et al., 2024). However, the relative values of decomposition rates and temperature sensitivities of POC versus MAOC under diverse ecosystems are unclear. Furthermore, both POC and MAOC have recently been integrated into soil carbon models, such as Millennial (Abramoff et al., 2022), MEND (Wang et al., 2015), and COMISSION (Ahrens et al., 2015). These soil carbon models have the assumption that MAOC has an upper limitation, i.e., MAOC saturation (Stewart et al., 2007; Castellano et al., 2015). However, the MAOC saturation concept is challenged by recent findings from a soil survey across Germany (Begill et al., 2023). Considering such debate, a recent study has proposed a POC-MAOC two-pool (PMoC) model with first-order equations to simulate the POC and MAOC dynamics (Zhou et al., 2024). However, the potential application of this model requires further validation.

Incubation experiments have been extensively employed as a powerful approach to the investigation of SOC decomposition, because this approach can offer the potential to isolate the specific effects from covariations in field (Feng et al., 2017). To quantify decomposition rates and their temperature sensitivity (Q_{10}) of specific SOC pools, experimental studies conduct incubation experiments separately for specific SOC pools. For example, Zheng et al. (2023) first fractionated SOC into POC and MAOC and then quantified the effect of nitrogen addition on the priming effects of POC and MAOC. Liu et al. (2022) measured the decomposition and Q_{10} of SOC in large macro-aggregate, small macro-aggregate, micro-aggregate, and silt plus clay particle, and found that the relative values of Q_{10} among soil aggregates were influenced by soil moisture. However, during SOC decomposition, SOC is transported among different SOC pools. In specific, once the POC is depolymerized by enzymes, some of the decayed POC would be absorbed by soil minerals (Lavallee et al., 2020). If soil minerals are removed from POC, all decayed POC would be taken up by microbial communities and then respired. In addition, during soil fractionation, the original microbial communities were remarkably altered. Therefore, it is urgent to develop a new approach to separate the decomposition rates and Q_{10} of POC and MAOC using bulk soil incubation data.

In this study, we proposed a method to separate the decomposition rates and Q_{10} for both POC and MAOC pools using a data set from a bulk soil incubation experiment. The data set was collected from five well-protected forest ecosystems across an altitudinal transect ranging from 841 m to 3445 m in the Eastern Himalayas. A 180-day incubation experiment was conducted to explore the decomposition rates of POC and MAOC. In addition, a continuous-flow incubation approach (Ding et al., 2016) was used to quantify the temperature response of decomposition; the data are reported in our recent publication (Hou et al., 2024). The PMoC model with first-order equations was used to simulate the decomposition and transformation processes of POC and MAOC (Zhou et al., 2024). The decomposition rates and Q_{10} for POC and MAOC were estimated directly through fitting the CO_2 emissions using the Bayesian Markov Chain Monte Carlo technique, which has been used to improve parameterization of ecological models (Hararuk et al., 2014).

2 Materials and methods

2.1 Soil incubation data

Soil samples were collected at Mount Namcha Barwa, which is located at the intersection of the Himalayas, Hengduan, and Nyenchenthanglha. The details of the studied site and soil information were described in our recent study (Hou et al., 2024). Briefly, soils in tropical montane evergreen broadleaved forest, subtropical montane evergreen broadleaved forest, temperate montane deciduous broadleaved forest, montane coniferous forest, and alpine timberline were collected along the altitudinal gradient at elevations of 841 m, 1547 m, 2488 m, 3348 m, and 3445 m, respectively.

A long-term incubation experiment lasting 180 days was conducted. The funnel-filter paper-drainage method was used to quantify the maximum water-holding capacity (Nelson et al., 2024). After that, 20 g of soil was placed in a 250 mL brown jar for a 7-day pre-incubation at 25°C in the dark, with 60% water-holding capacity. Following pre-incubation, CO_2 emission rates were recorded on days 1, 3, 5, 10, 15, 20, 30, 50, 70, 90, 120, 150, and 180. The water-holding capacity was monitored and adjusted by weighing the samples every three days throughout the pre-incubation and incubation periods. The CO_2 concentration was measured by gas chromatography (Agilent 7890B, USA). We also measured the POC and MAOC concentration after 180 days' incubation.

In addition, the data of the temperature response of decomposition (at 5°C, 10°C, 15°C, 20°C, and 25°C) and the corresponding methods of the continuous-flow incubation approach were provided in our recent study (Hou et al., 2024).

2.2 Model description

The PMoC model includes two SOC pools, i.e., POC and

MAOC (Zhou et al., 2024) (Fig. 1). The decomposition rates of POC and MAOC are represented by intrinsic decay constants of K_{P0} and K_{M0}, respectively. Decomposition of POC leads to respiration and formation of MAOC; the latter process was represented by the transformation coefficient of T_{PtoM}. Decomposition of MAOC leads to respiration and formation of POC; the latter process was represented by the transformation coefficient of T_{MtoP}. In specific, changes in POC and MAOC pools with time (t) are represented by the following equations:

$$\frac{\mathrm{dPOC}(t)}{\mathrm{d}t} = \mathrm{MAOC} \times K_{M0} \times T_{MtoP} - \mathrm{POC} \times K_{P0}, \quad (1)$$

$$\frac{\mathrm{dMAOC}(t)}{\mathrm{d}t} = \mathrm{POC} \times K_{P0} \times T_{PtoM} - \mathrm{MAOC} \times K_{M0}. \quad (2)$$

The temperature modifier for K_{P0} and K_{M0} is widely represented by a standard exponential relationship:

$$K_{PT} = K_{P0} \times Q_{10P}^{\frac{T-T_{ref}}{10}}, \quad (3)$$

$$K_{MT} = K_{M0} \times Q_{10M}^{\frac{T-T_{ref}}{10}}, \quad (4)$$

where T is the incubation temperature, T_{ref} represents the reference temperature (25°C). K_{PT} and K_{MT} are the decomposition rates of POC and MAOC at temperature T, which are modified by temperature sensitivities of POC (Q_{10P}) and MAOC (Q_{10M}).

2.3 Data assimilation

The parameters in the PMoC model were estimated by a Bayesian probabilistic inversion approach (Hararuk et al., 2014). In specific, the posterior probability density functions ($P(\theta|Z)$) of model parameters (θ) can be obtained by combining prior probability density functions for the parameters ($P(\theta)$) with the likelihood function ($P(Z|\theta)$):

$$P(\theta|Z) \propto P(Z|\theta)P(\theta). \quad (5)$$

The prior probability density functions were assigned uniform distributions by setting specific parameter ranges (Hararuk et al., 2014). The $P(Z|\theta)$ was estimated with the assumption that errors between observed and modeled respiration were independent of each other and followed a multivariate Gaussian distribution with a zero mean:

$$P(Z|\theta) \propto \exp\left\{\frac{(Y_{obs} - Y_{mod})^2}{2\sigma^2}\right\}, \quad (6)$$

where Y_{obs} and Y_{mod} are the observed and modeled respiration, while σ is the standard deviation of observation.

The probabilistic inversion was carried out using the Metropolis-Hastings algorithm, a Markov chain Monte Carlo technique, to construct the $P(\theta|Z)$. Briefly, the Metropolis-Hastings algorithm involves two primary steps: proposing and moving. In the proposing step, a new parameter set θ^{new} is proposed based on the previously accepted parameter set θ^{old} and a proposal distribution:

$$\theta^{new} = \theta^{old} + \frac{c \times (\theta_{max} - \theta_{min})}{S}, \quad (7)$$

where θ_{max} and θ_{min} are the maximum and minimum of model parameters, c is a random variable between −0.5 and 0.5, and S is used to control the proposing step size and is set to 5 (Xu et al., 2016). In the moving step, θ^{new} was tested against the Metropolis criterion to examine whether it should be accepted or rejected. The initial half of the accepted parameters was discarded and only the remaining parameters were used to calculate the $P(\theta|Z)$.

All the data sets and model codes were provided in the Supplementary materials.

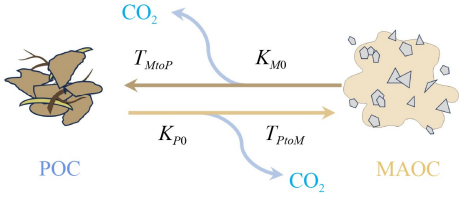

Fig. 1 Description of the PMoC model. POC, particulate organic carbon. MAOC, mineral-associated organic carbon. K_{P0}, intrinsic decay constant of POC. K_{M0}, intrinsic decay constant of MAOC. T_{PtoM}, proportion of POC that is transformed into MAOC. T_{MtoP}, proportion of MAOC that is transformed into POC.

3 Results and discussion

3.1 Decomposition rates of POC and MAOC

The positive correlation between observed and modeled CO_2 emissions ($y = 0.940\ x + 0.041$; $R^2 = 0.99$, $P < 0.001$) was strong, suggesting a good performance of the PMoC model in predicting SOC decomposition across 180-day incubation (Fig. 2(a)). After half a year of decomposition under favorable temperature and water conditions, although the pool size of POC continuously decreased (by 71.70%), the pool size of MAOC increased by 147% across the studied soils (Fig. 2(b)). In addition, our experimental measurement of MAOC after 180 days of decomposition also showed a significant increasing trend (Fig. 2(c)). Several previous experimental studies also found significant accumulation of MAOC and loss of POC during long-term incubation. For example, Gómez-Rey et al. (2010) showed that MAOC was increased by 26% after a 224-day incubation across the soils from five eucalypt plantations within a precipitation gradient in Portugal. The maximum accumulation of MAOC is up to

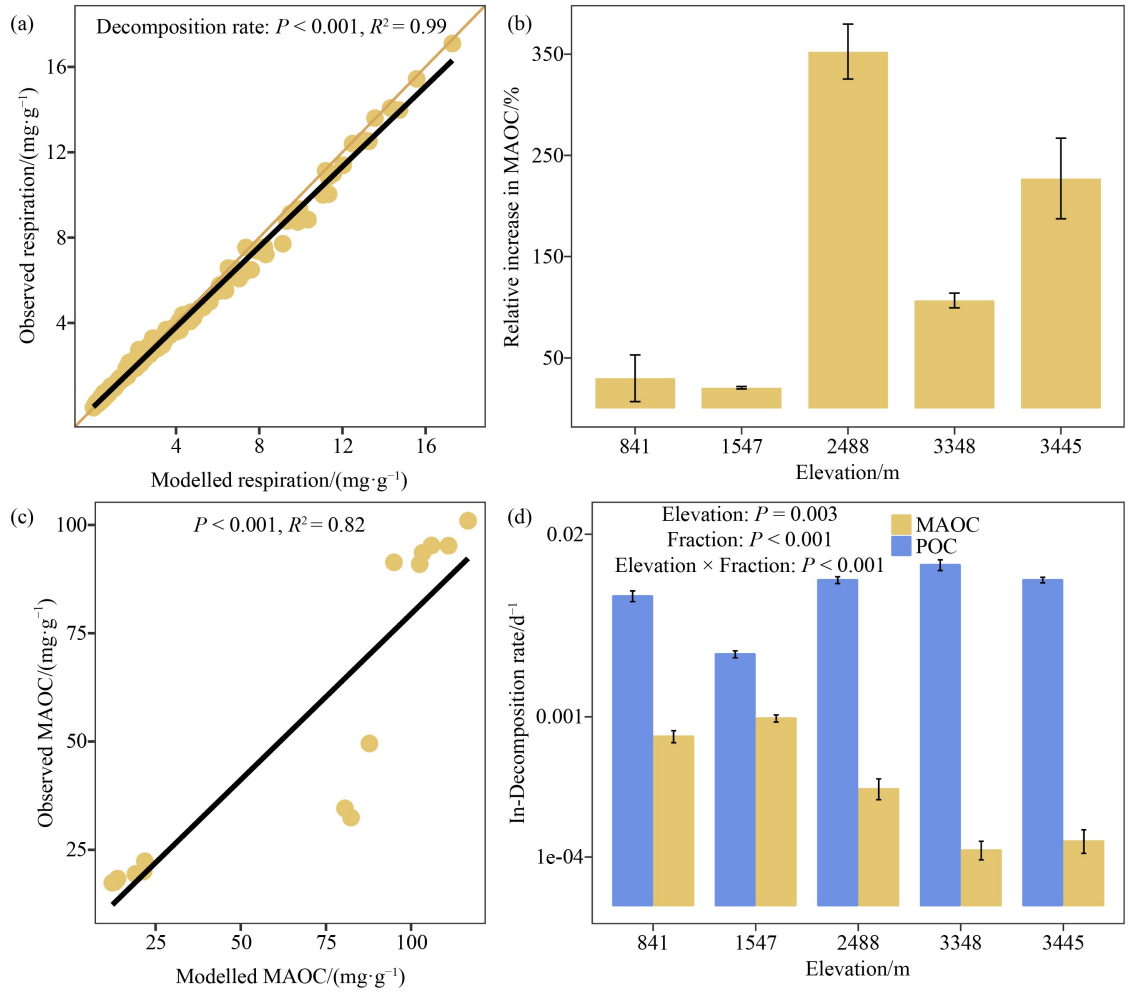

Fig. 2 Modeled decomposition of particulate organic carbon (POC) and mineral-associated organic carbon (MAOC). (a) The correlation between observed and modeled respiration. The brown line represents the 1:1 line. (b) Elevational variations in MAOC changes after half a year of decomposition from model. (c) The correlation between observed MAOC and modeled MAOC after half a year of decomposition. (d) Elevational variations in decomposition rates of POC and MAOC. Error bars represent the standard error. ln, natural log transform.

352% at an elevation of 2488 m (Fig. 2(b)). This huge accumulation of MAOC also challenged the concept of MAOC saturation, being coincided with a previous study (Begill et al., 2023).

Although the lack of fresh carbon input and high decomposition rate under comfortable temperature and water conditions, the accumulation of MAOC in laboratory incubation experiments drew attention to MAOC-destabilization in natural conditions (Bailey et al., 2019). First, the transformation of POC into MAOC is the result of adsorption of dissolved organic carbon onto soil minerals. The amount of dissolved organic carbon adsorption is a function of the final measured equilibrium solution concentration, maximum sorption capacity, and the binding affinity (Mayes et al., 2012). The leaching of dissolved organic carbon under field conditions results in a decreased organic carbon concentration, which consequently leads to a decrease in dissolved organic carbon sorption. Second, labile carbon inputs, especially for root exudates, result in the destabilization of existing MAOC via the priming effect (Begill et al., 2023). Oxalic acid, a common root exudate, can liberate organic compounds from protective associations with minerals for microbial uptake (Keiluweit et al., 2015). In addition, continuous fresh carbon input would keep a high level of microbial biomass under field conditions, contrasting with the decreasing trend of microbial biomass in incubation experiments (Ye et al., 2019). High microbial biomass would produce more siderophores, low-molecular-weight iron chelators, which can lead to the dissolution of well-crystallized ferric oxides such as goethite (Watteau and Berthelin, 1994; Collignon et al., 2012). Third, iron- and aluminum-bearing secondary minerals can quickly react to environmental changes (Collignon et al., 2012). Freeze–thaw cycles, drying-wetting cycles, and fluctuations of pH and redox can lead to destabilization of MAOC in field conditions (Bailey et al., 2019).

Reactive iron and aluminum oxides had a significant negative effect on the decomposition rate of MAOC but had no effect on decomposition rate of POC (Fig. 3). The adsorption of dissolved organic carbon onto the surfaces of reactive iron and aluminum oxides through electrostatic interactions, ligand exchange, hydrophobic interactions, hydrogen bonding, and cation bridging contributes to the formation of MAOC (Dong et al., 2023; Ren et al., 2024). Therefore, it is expected that there is a negative effect of reactive iron and aluminum oxides on the MAOC decomposition rate.

3.2 Q_{10} of POC and MAOC

The PMoC model with a standard exponential function also had good performance in predicting the temperature response of CO_2 emissions (correlation between observed and modeled CO_2 emissions: $y = 0.948x + 0.002$; $R^2 = 0.99$, $P < 0.001$; Fig. 4(a)). This is the first study to separate the bulk soil Q_{10} into Q_{10} for POC and Q_{10} for MAOC by a data-model fusion approach. According to the carbon quality temperature hypothesis, POC with high-molecular-weight polymeric material should be more sensitive to increasing temperature than MAOC with low-molecular-weight compounds (Craine et al., 2010). The significant interaction effect between elevation and SOC fractions on Q_{10} (Fig. 4(b)) suggested that the relative value of Q_{10} for POC versus MAOC is dependent upon elevations. Therefore, higher temperature sensitivity of MAOC decomposition than that of POC decomposition at elevations of 2488 m and 3445 m did not support the carbon quality temperature hypothesis. In addition, a lot of studies had also challenged the concept of carbon quality temperature hypothesis (Reynolds et al., 2017; Li et al., 2020; Liáng et al., 2023). Besides the laboratory incubation experiments, a large-scale field study also found that MAOC was more sensitive to climate change than POC in European grasslands and croplands (Lugato et al., 2021).

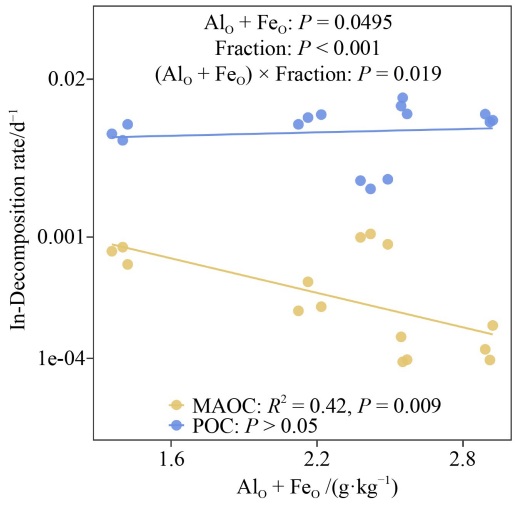

Fig. 3 Effects of reactive iron and aluminum oxides on the decomposition rates of particulate organic carbon (POC) and mineral-associated organic carbon (MAOC). $Al_O + Fe_O$, the sum of acid oxalate-extracted iron and aluminum oxides. ln, natural log-transform.

Although reactive iron plus aluminum oxides had no effect on the decomposition rate of POC, we found a significant interaction effect between reactive iron plus aluminum oxides and soil carbon fractions ($P = 0.030$) on Q_{10}, indicating a stronger negative effect of reactive iron plus aluminum oxides on temperature sensitivity of POC than that of MAOC decomposition (Fig. 5). Once the high molecular weight polymeric POC was depolymerized into low molecular weight dissolved organic carbon, the dissolved organic carbon would either

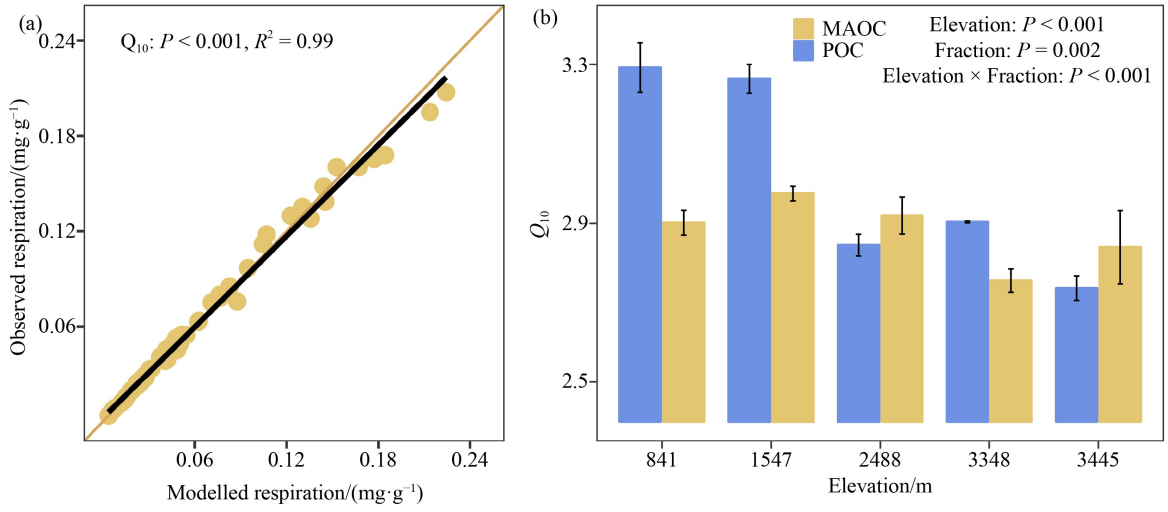

Fig. 4 Modeled temperature responses of particulate organic carbon (POC) and mineral-associated organic carbon (MAOC) decomposition. (a) The correlation between observed and modeled accumulated respiration. The brown line represents the 1:1 line. (b) Elevational variations in temperature sensitivities (Q_{10}) of POC and MAOC decomposition. Error bars represent the standard error.

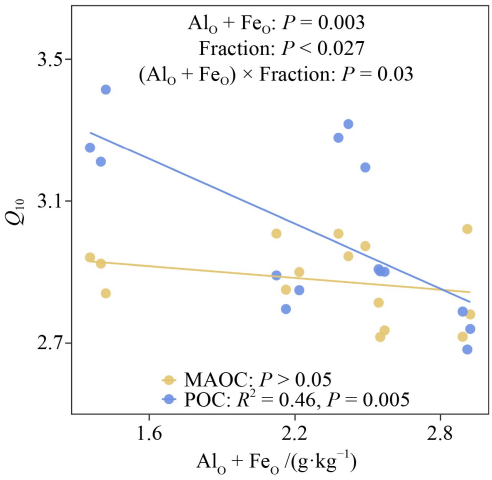

Fig. 5 Effects of reactive iron and aluminum oxides on temperature sensitivity (Q_{10}) of particulate organic carbon (POC) and mineral-associated organic carbon (MAOC) decomposition. $Al_O + Fe_O$, the sum of acid oxalate-extracted iron and aluminum oxides.

be respired by microbial communities or adsorbed by soil minerals under microcosm conditions. However, elevated temperature was found to reduce the formation efficiency of MAOC because of a high-temperature-induced increase in mineral crystallinity and a microbial-induced increase in Fe(III) reduction under warming conditions (Ren et al., 2024; Zhao et al., 2024). Therefore, the lower abundance of reactive iron plus aluminum oxides under high-temperature conditions would reduce the rate of dissolved organic carbon adsorption onto minerals (MAOC formation efficiency), which would increase the carbon availability for microbes and then result in a high Q_{10} for POC.

4 Conclusions

In summary, using the PMoC model and an incubation data set from a ~2600 m altitudinal transect in the Eastern Himalayas, we proposed an approach to separate the decomposition rates and temperature sensitivities of POC and MAOC from bulk soil using a data-model fusion approach. The PMoC model performed well in fitting the observed CO_2 emissions from a long-term decomposition incubation and from a short-term continuous-flow incubation. We found that reactive iron plus aluminum oxides inhibit the decomposition of MAOC rather than that of POC. However, the negative effect of reactive iron plus aluminum oxides on Q_{10} for POC is stronger than their effect on Q_{10} for MAOC. Overall, the proposed approach will improve our understanding of soil MAOC and POC dynamics using bulk soil incubation data.

Supplementary material is available in the online version of this article at http://dx.doi.org/10.1007/s11707-025-1161-2 and is accessible for authorized users.

Acknowledgments This work was financially supported by the National Key Research and Development Program of China (No. 2021YFD220 0401).

Competing interests The authors declare that they have no competing interests.

References

Abramoff R Z, Guenet B, Zhang H C, Georgiou K, Xu X F, Viscarra Rossel R A, Yuan W P, Ciais P (2022). Improved global-scale predictions of soil carbon stocks with Millennial Version 2. Soil Biol Biochem, 164: 108466

Ahrens B, Braakhekke M C, Guggenberger G, Schrumpf M, Reichstein M (2015). Contribution of sorption, DOC transport and microbial interactions to the ^{14}C age of a soil organic carbon profile: insights from a calibrated process model. Soil Biol Biochem, 88: 390–402

Bailey V L, Pries C H, Lajtha K (2019). What do we know about soil carbon destabilization. Environ Res Lett, 14(8): 083004

Begill N, Don A, Poeplau C (2023). No detectable upper limit of mineral-associated organic carbon in temperate agricultural soils. Glob Change Biol, 29(16): 4662–4669

Bossio D, Cook-Patton S, Ellis P, Fargione J, Sanderman J, Smith P, Wood S, Zomer R, von Unger M, Emmer I, Griscom B W (2020). The role of soil carbon in natural climate solutions. Nat Sustain, 3(5): 391–398

Buckeridge K M, Mason K E, McNamara N P, Ostle N, Puissant J, Goodall T, Griffiths R I, Stott A W, Whitaker J (2020). Environmental and microbial controls on microbial necromass recycling, an important precursor for soil carbon stabilization. Commun Earth Environ, 1(1): 36

Castellano M J, Mueller K E, Olk D C, Sawyer J E, Six J (2015). Integrating plant litter quality, soil organic matter stabilization, and the carbon saturation concept. Glob Change Biol, 21(9): 3200–3209

Collignon C, Ranger J, Turpault M P (2012). Seasonal dynamics of Al- and Fe-bearing secondary minerals in an acid forest soil: influence of Norway spruce roots (*Picea abies* (L.) Karst.). Eur J Soil Sci, 63(5): 592–602

Craine J M, Fierer N, McLauchlan K K (2010). Widespread coupling between the rate and temperature sensitivity of organic matter decay. Nat Geosci, 3(12): 854–857

Ding J Z, Chen L Y, Zhang B B, Liu L, Yang G B, Fang K, Chen Y L, Li F, Kou D, Ji C J, Luo Y Q, Yang Y H (2016). Linking temperature sensitivity of soil CO_2 release to substrate, environmental, and microbial properties across alpine ecosystems. Global Biogeochem Cycles, 30(9): 1310–1323

Dong H L, Zeng Q, Sheng Y Z, Chen C M, Yu G H, Kappler A (2023). Coupled iron cycling and organic matter transformation across redox interfaces. Nat Rev Earth Environ, 4(9): 659–673

Feng W T, Liang J Y, Hale L E, Jung C G, Chen J, Zhou J Z, Xu M G, Yuan M T, Wu L Y, Bracho R, Pegoraro E, Schuur E A G, Luo Y Q (2017). Enhanced decomposition of stable soil organic carbon

and microbial catabolic potentials by long‐term field warming. Glob Change Biol, 23(11): 4765–4776

García-Palacios P, Bradford M A, Benavente-Ferraces I, de Celis M, Delgado-Baquerizo M, García-Gil J C, Gaitán J J, Goñi-Urtiaga A, Mueller C W, Panettieri M, Rey A, Sáez-Sandino T, Schuur E A G, Sokol S W, Tedersoo L, Plaza C (2024). Dominance of particulate organic carbon in top mineral soils in cold regions. Nat Geosci, 17(2): 145–150

Gómez-Rey M X, Madeira M, Gonzalez-Prieto S J, Coutinho J (2010). Soil C and N dynamics within a precipitation gradient in Mediterranean eucalypt plantations. Plant Soil, 336(1−2): 157–171

Hararuk O, Xia J Y, Luo Y Q (2014). Evaluation and improvement of a global land model against soil carbon data using a Bayesian Markov chain Monte Carlo method. J Geophys Res Biogeosci, 119(3): 403–417

Heckman K, Hicks Pries C E, Lawrence C R, Rasmussen C, Crow S E, Hoyt A M, von Fromm S F, Shi Z, Stoner S, McGrath C, Beem-Miller J, Berhe A A, Blankinship J C, Keiluweit M, Marín-Spiotta E, Monroe J G, Plante A F, Schimel J, Sierra C A, Thompson A, Wagai R (2022). Beyond bulk: density fractions explain heterogeneity in global soil carbon abundance and persistence. Glob Change Biol, 28(3): 1178–1196

Hou L, Liang Y F, Wang C K, Zhou Z H (2024). Mineral protection explains the elevational variation of temperature sensitivity of soil carbon decomposition in the Eastern Himalaya. Appl Soil Ecol, 197: 105346

Jenkinson D, Coleman K (2008). The turnover of organic carbon in subsoils. Part 2. Modelling carbon turnover. Eur J Soil Sci, 59(2): 400–413

Keiluweit M, Bougoure J J, Nico P S, Pett-Ridge J, Weber P K, Kleber M (2015). Mineral protection of soil carbon counteracted by root exudates. Nat Clim Chang, 5(6): 588–595

Lavallee J M, Soong J L, Cotrufo M F (2020). Conceptualizing soil organic matter into particulate and mineral‐associated forms to address global change in the 21st century. Glob Change Biol, 26(1): 261–273

Lehmann J, Hansel C M, Kaiser C, Kleber M, Maher K, Manzoni S, Nunan N, Reichstein M, Schimel J P, Torn M S, Wieder W R, Kögel-Knabner I (2020). Persistence of soil organic carbon caused by functional complexity. Nat Geosci, 13(8): 529–534

Lehmann J, Kleber M (2015). The contentious nature of soil organic matter. Nature, 528(7580): 60–68

Li J Q, Nie M, Pendall E, Reich P B, Pei J, Noh N J, Zhu T, Li B, Fang C M (2020). Biogeographic variation in temperature sensitivity of decomposition in forest soils. Glob Change Biol, 26(3): 1873–1885

Liáng L L, Kirschbaum M U, Arcus V L, Schipper L A (2023). The carbon‐quality temperature hypothesis: fact or artefact. Glob Change Biol, 29(4): 935–942

Liu X T, Li Q, Tan S W, Wu X P, Song X J, Gao H Z, Han Z X, Jia A Y, Liang G P, Li S P (2022). Evaluation of carbon mineralization and its temperature sensitivity in different soil aggregates and moisture regimes: a 21-year tillage experiment. Sci Total Environ, 837: 155566

Lugato E, Lavallee J M, Haddix M L, Panagos P, Cotrufo M F (2021). Different climate sensitivity of particulate and mineral-associated soil organic matter. Nat Geosci, 14(5): 295–300

Mayes M A, Heal K R, Brandt C C, Phillips J R, Jardine P M (2012). Relation between soil order and sorption of dissolved organic carbon in temperate subsoils. Soil Sci Soc Am J, 76(3): 1027–1037

Nelson J T, Adjuik T A, Moore E B, VanLoocke A D, Ramirez Reyes A, McDaniel M D (2024). A simple, affordable, do-it-yourself method for measuring soil maximum water holding capacity. Commun Soil Sci Plant Anal, 55(8): 1190–1204

Parton W J, Hanson P J, Swanston C, Torn M, Trumbore S E, Riley W, Kelly R (2010). ForCent model development and testing using the Enriched Background Isotope Study experiment. J Geophys Res Biogeosci, 115: G04001

Ren S Y, Wang C K, Zhou Z H (2024). Global distributions of reactive iron and aluminum influence the spatial variation of soil organic carbon. Glob Change Biol, 30(11): e17576

Reynolds L L, Lajtha K, Bowden R D, Johnson B R, Bridgham S D (2017). The carbon quality-temperature hypothesis does not consistently predict temperature sensitivity of soil organic matter mineralization in soils from two manipulative ecosystem experiments. Biogeochemistry, 136(3): 249–260

Rovira P, Vallejo V R (2002). Labile and recalcitrant pools of carbon and nitrogen in organic matter decomposing at different depths in soil: an acid hydrolysis approach. Geoderma, 107(1−2): 109–141

Schmidt M W, Torn M S, Abiven S, Dittmar T, Guggenberger G, Janssens I A, Kleber M, Kögel-Knabner I, Lehmann J, Manning D A, Nannipieri P, Rasse D P, Weiner S, Trumbore S E (2011). Persistence of soil organic matter as an ecosystem property. Nature, 478(7367): 49–56

Stewart C E, Paustian K, Conant R T, Plante A F, Six J (2007). Soil carbon saturation: concept, evidence and evaluation. Biogeochemistry, 86(1): 19–31

Wang G S, Jagadamma S, Mayes M A, Schadt C W, Megan Steinweg J, Gu L H, Post W M (2015). Microbial dormancy improves development and experimental validation of ecosystem model. ISME J, 9(1): 226–237

Watteau F, Berthelin J (1994). Microbial dissolution of iron and aluminium from soil minerals: efficiency and specificity of hydroxamate siderophores compared to aliphatic acids. Eur J Soil Biol, 30(1): 1–9

Wiesmeier M, Urbanski L, Hobley E, Lang B, von Lützow M, Marin-Spiotta E, van Wesemael B, Rabot E, Ließ M, Garcia-Franco N, Wollschläger U, Vogel H J, Kögel-Knabner I (2019). Soil organic carbon storage as a key function of soils - A review of drivers and indicators at various scales. Geoderma, 333: 149–162

Xu X, Shi Z, Li D J, Rey A, Ruan H H, Craine J M, Liang J Y, Zhou J Z, Luo Y Q (2016). Soil properties control decomposition of soil organic carbon: results from data-assimilation analysis. Geoderma, 262: 235–242

Ye C L, Hall S J, Hu S J (2019). Controls on mineral-associated organic matter formation in a degraded Oxisol. Geoderma, 338:

383–392

Zhao J N, Feng X H, Hu J, He M, Wang S Y, Yang Y H, Chen L Y (2024). Mineral and microbial properties drive the formation of mineral-associated organic matter and its response to increased temperature. Glob Change Biol, 30(12): e70004

Zheng Y Y, Jin J, Wang X J, Clark G J, Franks A, Tang C X (2023). Nitrogen addition increases the glucose-induced priming effect of the particulate but not the mineral-associated organic carbon fraction. Soil Biol Biochem, 184: 109106

Zhou Z H, Liu L, Hou L (2022). Soil organic carbon stabilization and formation: mechanism and model. J Beijing For Univ, 44(10): 11–22

Zhou Z H, Ren C J, Wang C K, Delgado-Baquerizo M, Luo Y Q, Luo Z K, Du Z G, Zhu B, Yang Y H, Jiao S, Zhao F Z, Cai A D, Yang G H, Wei G H (2024). Global turnover of soil mineral-associated and particulate organic carbon. Nat Commun, 15(1): 5329